DESIGN AND EXPERIMENT OF IMPELLER TYPE VARIABLE FERTILIZER DISCHARGER DEVICE BASED ON EDEM SIMULATION
/
基于 EDEM 仿真的叶轮式变量排肥器设计与试验

Bai-wei Wang [1,2], Gang Che[*1,2], Lin Wan [*1,2], Nai-chen Zhao [1], Zhan-nan Guan [1]
[1)]College of Engineering, Heilongjiang Bayi Agricultural University, Daqing/P.R.China
[2)]Key Laboratory of Intelligent Agricultural Machinery Equipment in Heilongjiang Province, Daqing / P.R.China
Tel：+86-459-13836961617;E-mile: chegang180@126.com;
Corresponding author: Gang Che
DOI: https://doi.org/10.35633/inmateh-71-64

Keywords: *impeller-type, fertilizer discharger device, EDEM, variable, experiment*

ABSTRACT
Aiming at the problem of poor uniformity and stability of fertilizer discharge caused by the operation of the fertilizer discharger device in the variable fertilization operation of rice, combined with the agronomic requirements of deep fertilization on the northeast side, an impeller type variable side deep fertilizer was designed. According to the change of the prescription map, the adjustment factors are changed to achieve reasonable fertilization. Based on EDEM simulation, using the fertilizer discharge stability and uniformity coefficient of variation as indicators, under different impeller blades, different impeller speeds and different fertilizer discharge port angles, a secondary orthogonal rotation combination test was carried out, using Design-Expert. V8.0.6.1 is analyzed and tested, the regression equation and the response surface diagram are obtained, the interaction between the influencing factors is analyzed, and the best combination is determined. It is concluded that the stability and uniformity coefficient of variation of fertilizer discharge have reached the quality evaluation index of fertilization machinery. According to technical specifications, the variation coefficient stability of is 0.67%~2.85%, and the variation coefficient of uniformity is 2.7%~16.4%. When the number of blades is 6, the fan angle of the fertilizer outlet is 35.7°, and the impeller speed is 18.85 r·min^{-1}, the minimum variation coefficient of stability is 0.67%, and the minimum variation coefficient of uniformity is 2.1%. The bench test results are basically consistent with the optimal combination of simulation, and meet the design requirements.

摘要
针对在水稻变量施肥作业中，排肥器运转导致排肥均匀性和稳定性较差的问题。结合东北侧深施肥农艺要求，设计了一种叶轮式变量侧深施肥器。根据处方图变化，改变调节因素来实现合理施肥。基于 EDEM 模拟仿真，以排肥稳定性、均匀性变异系数为指标，在不同叶轮叶片、不同叶轮转速和不同排肥口角度大小参数下，进行二次正交旋转组合试验，运用 Design-Expert.V8.0.6.1 进行分析检验，得到回归方程和响应曲面图，分析影响因素之间交互作用，确定最佳组合，得出：排肥稳定性和均匀性变异系数均达到了施肥机械质量评价指标技术规范要求，稳定性变异系数为 0.67%~2.85%，均匀性变异系数为 2.7%~16.4%。当叶片数为 6 片，排肥口扇面角度大小为 35.7°，叶轮转速为 18.85 r·min^{-1} 时，稳定性变异系数最小为 0.67%，均匀性变异系数最小为 2.1%。台架实验结果与仿真最优组合基本吻合，符合设计要求。

INTRODUCTION
As rice is an important part of my country's food supply, it is particularly important to increase rice yield *(Shi et al., 2020)*. Fertilization is one of the main factors to increase crop yield. How to apply fertilizer reasonably has become a problem that cannot be ignored. Variable side-depth fertilization can carry out precise fertilization according to soil fertility, and achieve fertilizer saving and other effects *(Yuan et al., 2011; Mirzakhaninafchi et al., 2021; Cao., 1984)*. It solves the problems of inaccurate fertilization amount and low fertilizer utilization rate in the process of quantitative fertilization of rice, and achieves a good effect of weight loss and yield increase. The most critical part of the variable side-depth fertilization device is the fertilizer discharge device.

[1]*Bai-wei Wang, master degree; Gang Che, Prof. Ph.D.; Lin Wan, Prof. Ph.D.; Nai-chen Zhao, Ph.D.; Zhan-nan Guan master degree;*

The stability of the fertilizer supply, discharge and fertilization of the fertilizer discharge device determines its performance *(Wen et al., 2019)*. At present, the mainstream fertilizer discharge device at home and abroad include horizontal shaft type, horizontal turntable type, vibration type et al. *Bao et al., (2002), Ishola et al., (2014), Jun et al., (2021)*, most of them rely on forced fertilizer discharge, which will cause pulsation and fertilizer sticking inside the fertilizer discharge device resulting in inaccurate stability and uniformity of fertilizer discharge. Japan's Yanmar, Kubota, and Iseki respectively adopt horizontal hole-disk fertilizer discharge devices and outer grooved wheel-type dislocation fertilizer discharge device, which largely solve the pulse phenomenon in the fertilizer discharge process and improve accuracy and uniformity, but the structure is complex and difficult to maintain *(Zha et al., 2020; Cheng et al., 2012)*. Wang Jinfeng *(Wang et al., 2021)* designed the disc top-outside deep fertilization device for rice fields and Li Kai *(Li et al., 2017)* designed the dual-variable external groove wheel fertilizer discharge device. By adjusting the rotation impeller speed of the rotating shaft, the amount of fertilizer discharge can be changed, which improves the uniformity and stability of fertilization to a certain extent. However, in the process of work, pulsation occurs, resulting in inaccurate fertilizer application.

According to the agronomic requirements of side deep fertilization and the design technical requirements of fertilizer discharger device mechanism, the domestic side deep fertilization device has problems such as poor fertilization uniformity and stability. Combining with the characteristics of special granular fertilizer for side deep compound fertilizer commonly used in rice planting in Northeast China, an impeller-type variable side deep fertilizer is innovatively designed. Through the adjustment of fertilization amount, the fertilizer discharge device is studied by using EDEM software simulation, which provides a theoretical basis for the innovative development and optimization design of side deep fertilization equipment.

MATERIALS AND METHODS

Structure and working principle of fertilization device

The impeller-type variable fertilization device is shown in Fig. 1. It is mainly composed of a fertilizer box, an impeller-type fertilizer discharger device, a drive motor, an air delivery system, and a frame. The work flow chart of the whole machine is shown in Fig. 2.

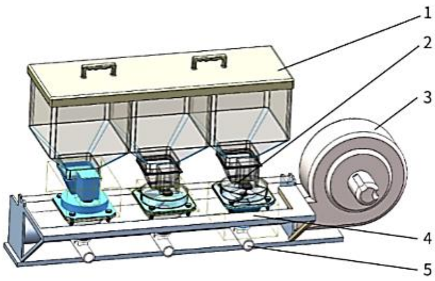

Fig. 1 - Wheeled variable fertilization device
1. Fertilizer box; 2. Impeller fertilizer discharge device ; 3. Fan; 4. Frame; 5: Venturi tube

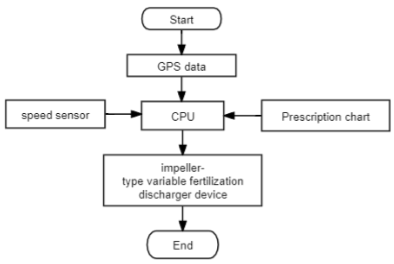

Fig. 2 - Work flow chart of the whole machine

The structure and working principle of the impeller type fertilizer discharger device

Impeller type fertilizer structure

The structure of the impeller type fertilizer discharger device mainly includes the upper casing, the impeller blade, the middle baffle, the lower casing, and the brush. The main components of the fertilizer discharger device structure are shown in Fig. 3.

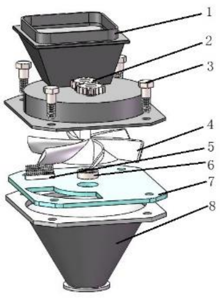

Fig. 3 - Three-dimensional drawing of the fertilizer discharger device component
1. Upper casing; 2. Transmission gear; 3. Fastening bolt; 4. Impeller blade; 5. Brush; 6. Bearing; 7. Middle baffle; 8. Lower casing

The working principle of fertilizer discharger device

When the fertilizer discharge device is in operation, fertilizers enter through the device inlet. The CPU, according to the prescription diagram information, converts PWM signals and transmits them to the discharge device motor. The discharge device motor achieves variable fertilization by adjusting the impeller speed, replacing different impellers, or adjusting the opening size of the central baffle in the fertilizer discharge port, in accordance with specified angles.

Granular Fertilizer Movement Analysis

Momentary Force Analysis of Fertilizer Particles Sliding During Fertilization

When the fertilizer falls to the fertilizer discharger device only the surface sliding on the impeller boss is considered. During the fertilizer filling process, the impeller rotates and the fertilizer fills the fertilizer discharger device cavity. Select a certain granular fertilizer A as the research object, and analyze it at a certain moment, assuming that the linear velocity of the fertilizer A is equal to the rotational linear velocity of the outer diameter of the blade, and taking the center of the impeller as the origin, a reference coordinate system OXYZ is established. The force analysis of granular fertilizer A is shown in Fig.4, the following relationship 1 is obtained:

$$F_A = G + F_N + F_f + F_c + F_e + F_b \tag{1}$$

In the formula：$G = m_A g, F_f = \mu m_A g, F_C = 2m_A \omega v_{rel}, F_e = m_A \omega^2 r$

where: F_A is the resultant force of granular fertilizer A, (N); G is the gravity of granular fertilizer A, (N); F_N is the support force of granular fertilizer A on the blade, (N); F_f is the friction force of granular fertilizer A on the impeller, (N) ; F_c is the Coriolis force, ((N); Fe is the traction centrifugal force, (N); m_A is the mass of the particle A, (g); ω is the angular velocity of the impeller, (r/min); r is the distance from the center of the impeller to the centroid of the fertilizer, (mm)；v_{rel} is the velocity relative to the boss, m/s.

The direction and magnitude of the interaction forces between granular fertilizers are constantly changing, but there is a mutual interaction force between the particles. At this point, an equilibrium state is reached, and the interaction force between the fertilizers is zero. During the sliding moment of granular fertilizer A, A is stationary relative to the convex surface, with v_{rel} being zero, meaning F_C is zero. At this moment, the resultant force acting on the fertilizer is described by the following equation:

$$F_A = G + F_N + F_f + F_e \tag{2}$$

At this time, it is assumed that the direction of the friction force received is opposite to the direction of motion. The angle between the friction force and the XOZ plane is set to γ, and the analysis shows that the larger the γ, the smaller the slip along the Z axis. The force analysis of granular fertilizer A is shown in Fig. 4.

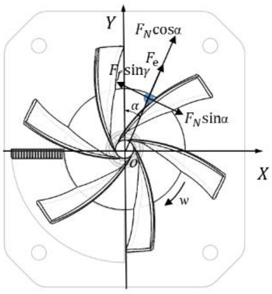

（a）

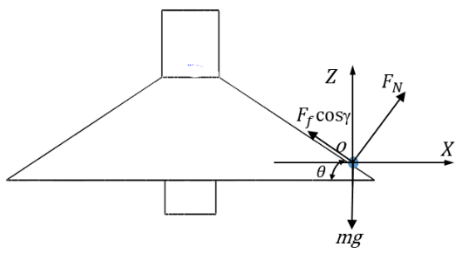

（b）

Fig. 4 - Instantaneous force analysis of fertilizer particles sliding during fertilization process

Analyzing the fertilizer particle A at the sliding instant equation is 3, 4, 5:

$$F_e + F_N \cos\alpha = 0 \tag{3}$$

$$F_N \sin\alpha - F_f \sin\gamma = 0 \tag{4}$$

$$F_f \cos\gamma \cos\theta + F_N \sin\theta - G = 0 \tag{5}$$

Simplified processing:

$$\gamma = \arctan\frac{r\omega^2 \sin\alpha\cos\theta}{g\cos\alpha - r\omega^2 \sin\theta} \tag{6}$$

where: θ is the bottom angle of the impeller boss, (°); α is the initial angle of fertilizer sliding, (°); γ is the angle between the friction force and the XOZ plane, (°)

According to the kinetic energy theorem, analyze the possible maximum relative velocity, take the projection form of the particle center of mass motion differential equation on the coordinate axis, and establish the motion equation:

$$m\frac{d_v}{d_t} = mg\sin\alpha - \mu mg\cos\alpha \tag{7}$$

The larger the γ, the more parallel the fertilizer movement track is to the Y-axis direction, the easier it is to enter the fertilizer discharger device cavity, and the smaller the slippage along the Z-axis is. On the contrary, the greater the Z-axis slippage, the fertilizer will have slippage fluctuations, which will affect the filling factor. It can be seen from formulas 6 and 7 that γ is related to ω (impeller speed n), bottom angle θ of impeller boss, initial angle α when fertilizer begins to slide, and distance r from impeller center to fertilizer center of mass. Therefore, appropriately increasing the rotational impeller speed ω helps to improve the uniformity and stability of fertilization.

Momentary Force Analysis of Sliding Granular Fertilizer during Fertilizer Discharging

When the fertilizer reaches the fertilizer outlet of the middle baffle, the fertilizer moves flat and the impeller speed when it leaves the impeller is the impeller tangential fertilizer speed V_A, and falls to the lower casing under the joint action of its own gravity G, centrifugal force F_e and air resistance F_f, decompose V_A into V_X, V_y, and its horizontal displacement X and vertical displacement Y are shown in Fig. 5

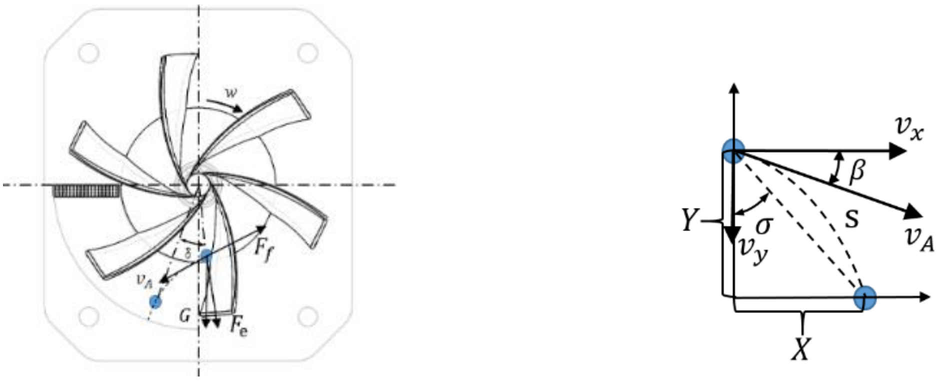

(a) (b)

Fig. 5 - Analysis of fertilizer particle discharge port movement in fertilizer discharge process

$$\begin{cases} X = v_x t \\ Y = v_y t \\ Z = \frac{1}{2}gt^2 \end{cases} \tag{8}$$

$$v_A = \omega r \tag{9}$$

$$v_x = v_A\cos\beta \tag{10}$$

$$v_y = v_A\sin\beta \tag{11}$$

Where: X is the x displacement of the fertilizer particle A in the horizontal direction, (m); Y is the y displacement of the fertilizer particle A in the horizontal direction, (m); Z is the z displacement of the fertilizer particle A in the vertical direction, (m); v_x is the movement of the fertilizer particle A in the horizontal direction. The velocity in the x direction per hour, (m/s); v_y is the velocity in the y direction of the fertilizer particle A when it is thrown flat, (m/s); g is the acceleration of gravity, (m/s^2); t is the time for the fertilizer particle A to do flat throwing motion, (s); ω is the angular velocity of the impeller blade, (rad/s); r is the distance from the center of the impeller to the center of mass of the fertilizer, (mm).

According to Newton's second law, when the fertilizer is thrown, the trajectory is a parabola, and the differential equation of motion is established:

$$\begin{cases} m\frac{d^2x}{dt} = 0 \\ m\frac{d^2}{dt} = mg \end{cases} \tag{12}$$

When t=0, X=0, $m\frac{d^2x}{dt} = v_x$; when t=0, y=0, $m\frac{d^2x}{dt} = 0$

According to the motion equations 8~12 of the granular fertilizer, the trajectory equation of motion is:

$$Z = \frac{g}{2v_x^2}x^2 \tag{13}$$

$$\delta = \arctan\frac{X}{Y+r} = arctan\frac{\omega r\cos\sqrt{\frac{2Z}{g}}}{\frac{s\omega}{\sigma}\sqrt{\frac{2Z}{g}}+r} \tag{14}$$

Where: δ is the starting and ending position rotation angle of the fertilizer, (°); σ is the offset angle of the fertilizer flat throwing, (°); s is the length of the fertilizer flat throwing trajectory, (mm).

The position of the fertilizer drop point is related to the rotation angle δ, and the rotation angle δ is related to the angular velocity ω, the fertilizer rotation angle σ, and the vertical displacement Z. When the fertilizer rotation angle σ and the vertical displacement Z are constant, as the rotational impeller speed n increases, the falling δ will also increase. The larger the δ, the easier it is for the fertilizer to accumulate and cause blockage. Therefore, appropriately increasing the impeller speed can improve the performance of fertilizer discharge.

EDEM simulation test analysis

The fertilizer used in this paper is domestic compound fertilizer, the raw material of the fertilizer discharger device is transparent PVC hard plastic, and the 3D printing material used in the test is PLA. Compared with PLA, PVC has a shorter service life and is prone to problems such as wear and aging, and 3D printing is more accurate and convenient. The brush is made of nylon 66. Through consulting the literature *(Tormi et al., 2022; Xing et al., 2019; Tai et al., 2020; Gao et al., 2019)* and related experiments, the size parameters of the fertilizer and the characteristic parameters of various materials are obtained as shown in Table 1.

The average length, width, and height of the compound fertilizer are 4.66 mm, 4.31 mm, and 3.92 mm, and the equivalent diameter is 4.28 mm. The average spherical rate is 95%, and the density is 1670 kg/m^3.

Table 1

Compound fertilizer and geometry simulation parameters

Item	Property	Value	Item	Property	Value
fertilizer	Poisson's ratio	0.25	Granules-Granules	rolling friction coefficient	0.28
	Shear modulus	1.0X10^7		static friction coefficient	0.48
	Density kg/m^3	1670		Recovery coefficient	0.52
PLA	Poisson's ratio	0.35	Fertilizer-PLA	rolling friction coefficient	0.18
	Shear modulus	4.0X10^8		static friction coefficient	0.23
	Density kg/m^3	1255		Recovery coefficient	0.51

RESULTS

After importing the fertilizer discharge device into the EDEM software, an analysis was conducted on the fertilizer angular velocity, fertilizer velocity, and forces acting on the fertilizer for impeller speeds of 10 m/s and 20 m/s, respectively. The changing status can be visually observed through the color and data bars of the fertilizer, as depicted in Figures 6 and 7.

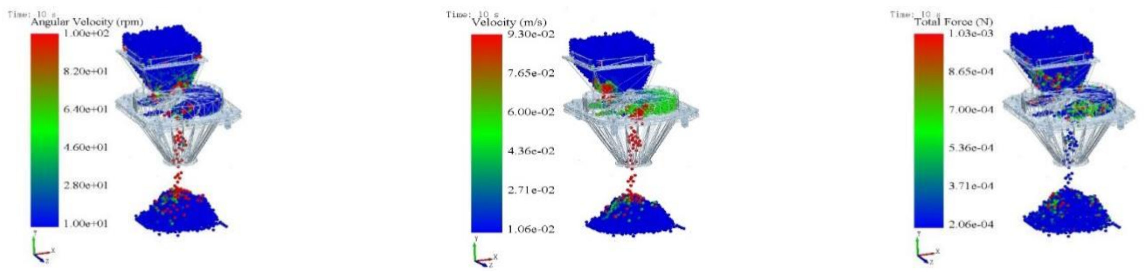

（a） （b） （c）

Fig. 6 - The angular velocity, velocity and force model of the fertilizer when the impeller speed is 10 r/min

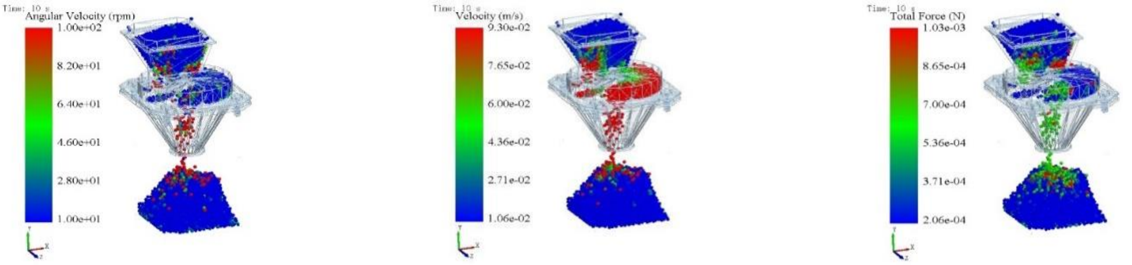

（a） （b） （c）

Fig. 7 - The angular velocity, velocity and force model of the fertilizer when the impeller speed is 20 r/min

It can be seen from Figs. 6 and 7 that the angular velocity, velocity, and force of the fertilizer vary greatly when the fertilizer inlet contacts the impeller and when the impeller discharges the fertilizer from the fertilizer outlet, while the other places have no obvious variation range. According to the angular velocity model, with the increase of the impeller speed, the fertilizer angular velocity ranges from 10 ~ 100 r/min when the variation range is large. The fertilizer speed model shows that the fertilizer speed range of the large change is concentrated inside the fertilizer discharger device cavity. With the increase of the impeller speed, the speed of the fertilizer also increases, and the range is $1.06\times10^{(-2)}$ ~ $9.3\times10^{(-2)}$ m/s. According to the fertilizer force model, with the increase of the impeller speed, when the fertilizer inlet contacts the impeller and when the impeller discharges the fertilizer from the fertilizer discharge port, the greater change is in the range of $2.06\times10^{(-4)}$ ~ $1.03\times10^{(-3)}$ N. Compared with other rotational impeller speeds, the angular velocity, velocity, and force of the fertilizer have no major changes in places where the variation range is large. With the increase of the impeller speed, the angular velocity, velocity, and force of the fertilizer all increase.

Simulation experiment design and analysis

Use Setup Selections in Analyst to construct Grid Bin grid *(Wang et al., 2023; Dang et al., 2022),* refer to NY/T 1003-2006 "Technical Specifications for Quality Evaluation of Fertilizer Machinery" standard, design experiments, calculate the variation coefficient of fertilizer discharge stability and the uniformity variation of fertilizer discharger device coefficient.

Central Composite Design

Domestic compound fertilizers were selected to carry out three-factor five-level quadratic rotation combination design experiments, and the optimum working parameter combination was obtained through significance analysis. During the simulation process, without the influence of other environmental factors, according to the rice fertilization rate of 300-675 kg/ha, the number of leaves is selected to be 2~6 pieces, the fan angle of the fertilizer outlet is 30~70°, and the impeller speed is 5~25 r min^{-1}. The factor code table is Table 2, the test program design and results are shown in Table 3, X_1, X_2, X_3 in the table are the number of blades, the fan angle of the fertilizer discharge port and the code value of the impeller speed, Y_1, Y_2 are the coefficient of variation of fertilizer discharge stability and the fertilizer uniformity variation coefficient.

Table 2

Experiment factor coding

coding	factor		
	Number of blades X_1/[piece]	Fan angle of fertilizer outlet X_2/[°]	impeller Speed X_3/[r·min^{-1}]
1.682	6	70	25
1	5	60	20
0	4	50	15
-1	3	40	10
-1.682	2	30	5

According to the design of the test coding table, conduct a simulation test and fill in the test results in Table 3.

Table 3

Experimental design and results

coding	Number of blades X_1/[piece]	Fan angle of fertilizer outlet X_2/[°]	impeller Speed X_3/[r·min^{-1}]	Coefficient of variation Y_1 of fertilizer discharge stability [%]	Fertilizer uniformity variation coefficient Y_2 [%]
1	-1	-1	-1	0.85%	5.68%
2	1	-1	-1	1.72%	12.38%
3	-1	1	-1	1.34%	2.73%
4	1	1	-1	2.13%	16.44%
5	-1	-1	1	2.46%	4.72%
6	1	-1	1	1.72%	4.34%
7	-1	1	1	1.32%	8.82%
8	1	1	1	1.29%	3.13%
9	-1.68	0	0	1.01%	5.01%
10	1.68	0	0	2.84%	16.33%
11	0	-1.68	0	1.36%	4.40%
12	0	1.68	0	1.18%	3.19%
13	0	0	-1.68	0.82%	13.43%
14	0	0	1.68	3.29%	2.86%
15	0	0	0	1.56%	4.53%
16	0	0	0	1.76%	2.76%
17	0	0	0	2.36%	6.39%
18	0	0	0	1.25%	9.98%
19	0	0	0	3.09%	5.71%
20	0	0	0	1.23%	5.81%
21	0	0	0	1.75%	9.98%
22	0	0	0	3.78%	5.42%
23	0	0	0	1.54%	3.45%

Analysis of test results

The software Design-Expert.V8.0.6.1 was used to carry out multiple regression fitting analysis on the experimental results, and the regression equation between the factors and between the coefficient of variation of stability and the coefficient of variation of uniformity was established. The results of variance analysis and significance are shown in Table 4. For the stability coefficient of variation, the model significance test $p<0.01$ indicates that the model is statistically significant. The first-order item X_1, the second-order item $X_1 X_3$ have a very significant impact ($P<0.01$), the second-order item X_3^2 has a significant impact ($P<0.05$), and the lack-of-fit P value is 0.332>0.05, which is beneficial to the model, there is no lack of fit factor, and the fitting degree is good. For the coefficient of variation for homogeneity, the model significance test $p<0.01$, indicates that the model is statistically significant. The first-order items X_1, X_3, the second-order items $X_1 X_3$ have a very significant impact ($P<0.01$), and the second-order items X_1^2 has a significant influence ($P<0.05$), and the lack of fit P value is 0.4467>0.05, which is beneficial to the model. There is no lack of fit factor, and the degree of fitting is good. This regression equation can be used instead of the real point of the test to analyze the experimental results.

Table 4

Analysis of Regression Equations ANOVA

source of variance	stability coefficient of variation				uniformity coefficient of variation			
	sum of square	degrees of freedom	F	P	sum of square	degrees of freedom	F	P
Model	4.974E-004	9	4.57	0.0069	0.031	9	5.30	0.0037
X_1	1.524E-004	1	12.62	0.0035	8.167E-003	1	12.41	0.0037
X_2	1.832E-005	1	1.52	0.2400	2.829E-005	1	0.043	0.8390
X_3	1.183E-005	1	0.98	0.3404	8.460E-003	1	12.85	0.0033
X_1X_2	1.914E-005	1	1.58	0.2303	3.583E-005	1	0.054	0.8192
X_1X_3	1.148E-004	1	9.50	0.0087	8.762E-003	1	13.31	0.0029
X_2X_3	4.327E-005	1	3.58	0.0809	3.954E-005	1	0.060	0.8102
X_1^2	4.290E-005	1	3.55	0.0821	3.960E-003	1	6.02	0.0291

source of variance	stability coefficient of variation				uniformity coefficient of variation			
	sum of square	degrees of freedom	F	P	sum of square	degrees of freedom	F	P
X_2^2	7.232E-006	1	0.60	0.4529	1.158E-003	1	1.76	0.2075
X_3^2	8.675E-005	1	7.18	0.0189	7.444E-004	1	1.13	0.3069
Residual	1.570E-004	13			8.557E-003	13		
Lack of fit	7.219E-005	5	1.36	0.332	3.412E-003	5	1.06	0.4467
Pure error	8.486E-005	8			5.145E-003	8		
Sum	6.544E-004	22			0.040	22		

Note: * indicates significant impact (P <0.05) and ** indicates very significant impact (P <0.01).

Carry out quadratic response surface regression analysis, remove insignificant factors, and obtain the following multivariate quadratic response surface regression model:

$$Y_1(\%) = 0.016 + 3.34 \times 10^{-3}X_1 + 3.79 \times 10^{-3}X_1X_3 - 2.37 \times 10^{-3}X_3^2 \quad (15)$$

$$Y_2(\%) = 0.060 + 0.024X_1 - 0.025X_3 - 0.033X_1X_3 - 6.84 \times 10^{-3}X_1^2 \quad (16)$$

Response Surface and Interaction Analysis

The coefficient of variation of fertilizer discharge stability and the coefficient of variation of fertilizer discharge uniformity are important indicators to measure the fertilizer discharger device. The influence of the interaction of various factors on the stability coefficient of variation is analyzed, and the corresponding mathematical model is obtained. For example, Table 5 shows the interactive effects of various factors on the coefficient of variation of fertilizer discharge stability. Fig. 8 shows the response surface analysis diagram of each factor on the coefficient of variation of fertilizer discharge stability. Table 6 shows the interaction of various factors on the coefficient of variation of fertilizer discharge uniformity. Interaction effects, as shown in Fig. 9 is the response surface analysis diagram of each factor on the coefficient of variation of fertilizer uniformity.

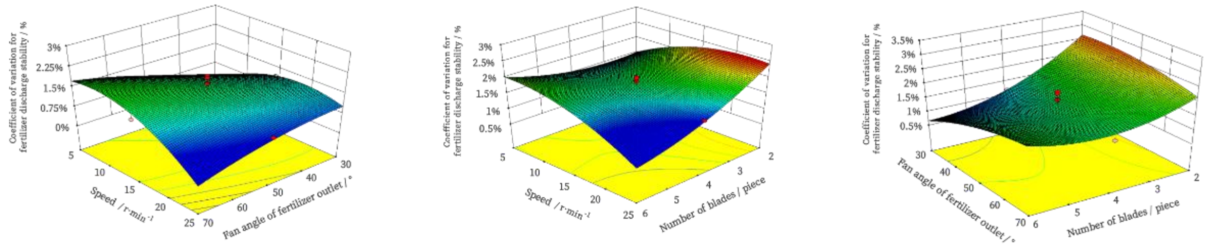

（a） （b） （c）

Fig. 8 - Effect of interactions on stability coefficient of variation

Table 5

Interaction of factors on coefficient of variation of fertilizer discharge stability

Coefficient of variation Y_1 of fertilizer discharge stability Y_1	Number of blades X_1/(piece)	Fan angle of fertilizer outlet X_2/(°)	impeller speed X_3/ (r·min^{-1})	Value range of Y_1min factor
decrease	4	increase	constant	50-X2-70°
decrease	4	constant	increase	15–X3-25 r·min^{-1}
decrease	increase	50	constant	4-X1-6 piece
decrease	constant	50	increase	15–X3-25 r·min^{-1}
decrease	increase	constant	15	4-X1-6 piece
increase	constant	increase	15	30-X2-50°

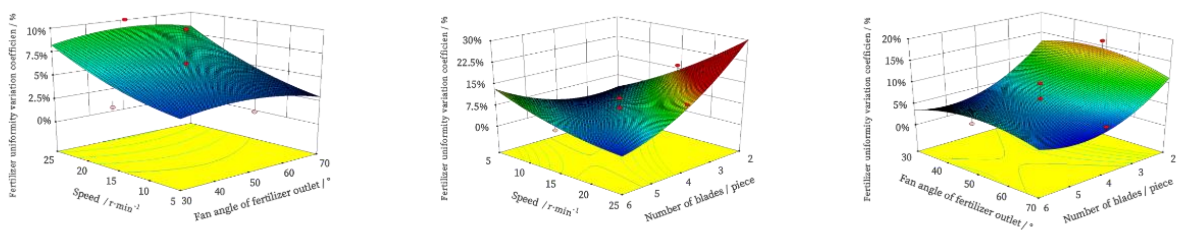

(a) (b) ©

Fig. 9 - The effect of interaction on uniformity

Table 6

Interaction of factors on coefficient of variation of fertilizer discharge uniformity

Coefficient of variation of uniformity Y_2	Number of blades X_1/(piece)	Fan angle of fertilizer outlet X_2/(°)	impeller speed X_3/ （$r \cdot min^{-1}$）	Value range of Y_2min factor
Decrease after increase	4	increase	constant	50-X_2-70°
increase	4	constant	increase	5–X_3-15 $r \cdot min^{-1}$
increase	2-4	50	5-15	4-X_1-6 piece
decrease	5、6		15-25	15–X_3-25 $r \cdot min^{-1}$
increase after decrease	increase	constant	15	3-X_1-5 piece
Decrease after increase	constant	increase	15	50-X_2-70°

Experimental optimization

Utilizing Design-Expert.V8.0.6.1 software for optimization, a mathematical model represented by equation (17) was established to determine the optimal combination of factors. Through calculations, it was found that when the number of blades is 6, the fan angle of the fertilizer outlet is 35.7°, and the impeller speed is 18.85 $r \cdot min^{-1}$, the minimum coefficient of stability variation is 0.67%, and the minimum coefficient of uniformity variation is 2.1%.

$$\begin{cases} \min Y_1 \\ \min Y_2 \\ s.t \begin{cases} 2 \le X_1 \le 6 \\ 30° \le X_2 \le 70° \\ 5 \le X_3 \le 25 \\ 0 \le Y_1(X_1、X_2，X_3) \le 1 \\ 0 \le Y_2(X_1、X_2，X_3) \le 1 \end{cases} \end{cases} \tag{17}$$

Bench test

The experiment site is the seeding laboratory of Heilongjiang Bayi Agricultural Reclamation University, the fertilizer is Stanley compound fertilizer, and a self-made fertilizer discharge device is used. During the experiment, the fertilizer discharge device is installed on the test bench, and the test factors of the fertilizer discharge device adopt the optimal combination of simulation, the middle baffle and blades are 3D printed, and the motor speed is precisely controlled by a single-chip microcomputer. The fertilizer discharge performance test bench is shown in the Fig. 10.

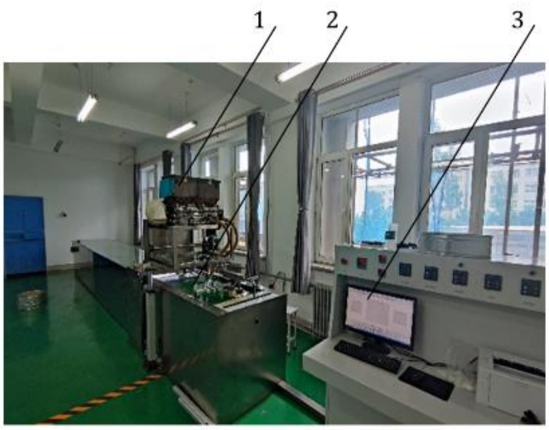

Fig. 10 - Test bench of impeller fertilization device

1. Seed-discharging performance test bench 2. Fertilizer device 3. Fertilizer collection belt

During the stability test, the conveyor belt does not rotate. The collection box below the fertilizer discharger device collects the fertilizer mass for 15 s, repeats 5 times, and takes the average value. Calculate the coefficient of variation for stability.

In the uniformity test, the conveyor belt speed of the test bench was 1 $m \cdot s^{-1}$, and 30 continuous sections of 10 cm fertilizer mass were collected, repeated 5 times, and the average value was taken to calculate the uniformity coefficient of variation. The experimental results are shown in the table 7.

Table 7

Test results

Number of experiments	Coefficient of variation Y_1 of fertilizer discharge stability [%]	Fertilizer uniformity variation coefficient Y_2 [%]
1	1.56	4.65
2	0.89	7.32
3	2.65	6.55
4	3.28	5.23
5	2.11	4.98
average value	2.098	5.746

Bench test results show that the coefficient of variation of fertilizer discharger device stability is 2.098%, and the coefficient of variation of uniformity is 5.746%. The simulation results are basically consistent with the bench results and meet NY/T 1003-2006 "Technical Specifications for Quality Evaluation of Fertilizer Machinery" Standards to meet fertilization requirements.

CONCLUSIONS

In addressing the challenges of poor fertilizer uniformity and stability resulting from the operation of the fertilizer discharger device in variable-rate fertilization for rice, a blade-type variable-rate fertilizer discharger device was designed. The key component structural parameters of the blade-type discharger device and the instantaneous processes of filling and discharging fertilizer were analyzed to identify the factors influencing the discharger device's performance.

Through EDEM discrete element simulation, a Central Composite Design was employed to investigate the effects of impeller speed, fan angle of fertilizer outlet, and number of blades. Utilizing Design-Expert.V8.0.6.1 software for optimization analysis, both the stability and uniformity coefficients of variation for fertilizer discharge met the technical specifications required for the mechanical quality assessment of the fertilization equipment. The stability coefficient of variation ranged from 0.67% to 2.85%, while the uniformity coefficient of variation ranged from 2.7% to 16.4%.

Taking the number of blades, the fan angle of the fertilizer outlet, and the speed of the impeller as the influencing factors, the variation range of each factor is determined, and the regression equation is obtained through analysis. Combined with the change trend of the response surface method, after the optimization module is processed, it is obtained: when the number of blades is 6, the fan angle of the fertilizer outlet is 35.7° and the impeller speed is 18.85 $r \cdot min^{-1}$, the coefficient of variation of the stability is 0.67%, and the coefficient of variation of the uniformity is at least 2.1%. The bench test verification results are basically consistent with the simulation results and meet the design requirements.

ACKNOWLEDGEMENT

The authors were funded by the China Central Government's Special Project for Guiding Local Science and Technology Development (ZY20B05); the National Grassroots Agricultural Technology Promotion Project (NJ202105); and the Heilongjiang Provincial Natural Science Foundation Project (LH2022E098).

REFERENCES

[1] Bao, B.Q., Long-Ze, A. N., Feng-Ying, H.U. (2002). The rice field mechanization state in Japan, China and other countries (我国和日本等国水田机械发展概况). *Journal of Agricultural Mechanization Research.* Vol. 03, pp.23-25. Heilongjiang/China.

[2] Cao, R.D. (1984). Experimental research on disc fertilizer discharger device (盘式排肥器的试验研究). *Journal of Agricultural Machinery*, Vol. 03, pp.74-81. Jiangsu/China.

[3] Cheng, C.H., Xu, C.L., Bi, C.H., & Zhang, X.D. (2012). Research on side deep fertilization technology and device of rice transplanter (水稻插秧机侧深施肥技术及装置的研究). *Journal of Heilongjiang Bayi Agricultural Reclamation University*, Vol. 06, pp. 10-12+25. Heilongjiang/China.

[4] Dang, Y., Yang, G., Wang, J., Zhou, Z., & Xu, Z. (2022). A Decision-Making Capability Optimization Scheme of Control Combination and PID Controller Parameters for Bivariate Fertilizer Applicator Improved by Using EDEM. *Agriculture*, Vol. *12*(12), pp. 2100. Henan/China.

[5] Gao, G.B. (2019). *Design and experiment of key components of wind-driven rice side-deep fertilizer discharger device* (风送式水稻侧深施肥装置关键部件设计与试验), Master's thesis, Northeast Agricultural University. Heilongjiang/China.

[6] Ishola, T. A., Yahya, A., Shariff, A. R. M., & Aziz, S. A. (2014). A novel variable rate pneumatic fertilizer applicator. *Instrumentation Science & Technology,* Vol. 42(4), pp. 369-384. Malaysia

[7] Jun, L., Dequan, Z., Qilei, T., Congyang, Y., Tingjue, W., Kang, X., ... & Juan, L. (2021). Design and experiment of adjustable socket-wheel precision fertilizer apparatus for dry direct-seeding rice. *INMATEH-Agricultural Engineering*, Vol. 63(1), pp. 121-130. Anhui/China.

[8] Li, K. (2017). *Design and research of variable fertilization system* (变量施肥系统的设计与研究) Master's thesis, Shihezi University. Xinjiang/China.

[9] Mirzakhaninafchi, H., Singh, M., Bector, V., Gupta, O. P., & Singh, R. (2021). Design and development of a variable rate applicator for real-time application of fertilizer. *Sustainability*, Vol. 13(16), pp. 8694. India

[10] Shi, Y., Zhu, Y., Wang, X., Sun, X., Ding, Y., Cao, W., & Hu, Z. (2020). Progress and development on biological information of crop phenotype research applied to real-time variable-rate fertilization. *Plant methods*, Vol. 16, pp. 1-15, England.

[11] Tai, Q.L. (2020). *Design and experiment of adjustable socket wheel precision fertilizer discharger device* (可调窝眼轮式精量排肥器设计与试验), Master's thesis, Anhui Agricultural University. Anhui/China

[12] Tormi, I., Märt, R., Indrek, V., & Jüri, O. (2022). Feasibility analysis of fluted roller dispenser application for precision fertilization. *INMATEH-Agricultural Engineering*, Vol. 68(3), pp. 415-423. Estonia

[13] Wang, J.F., Shang, W.H., Weng, W.X., & Chen, X.S. (2021). Design and experiment of side-deep fertilization device for rice fields with disc ejector (圆盘顶出式水田侧深施肥装置设计与试验). *Journal of Agricultural Machinery*, Vol. 06, pp. 62-72. Heilongjiang/China.

[14] Wang, J.F., Fu, Z.D., Weng, W. X., & Yang, D.G..(2022). Design and experiment of double-row fertilizer for side-deep fertilization of rice fields with conical disc push plate (圆锥盘推板式水田侧深施肥双行排肥器设计与试验). *Journal of Agricultural Machinery*, Vol. 02, pp. 53-62+106, Heilongjiang/China.

[15] Wen, X., Ya.X.H. (2019). Design and parameter optimization of key components of organic fertilizer spreader (有机肥撒播机关键部件设计及参数优化). A*gricultural Machinery Use and Maintenance* Vol.06, pp. 25. Guangxi/China

[16] Xing, X.P. (2019). *Research on two-stage screw-driven fertilizer discharge and deep fertilizer discharger device in rice fields* (水田双级螺旋驱动的排肥与深施肥装置研究) Master's thesis, South China Agricultural University. Guangdong/China.

[17] Yuan, W.S., Mei, J., Chong you, W., Ti Giong, X. (2011). Development status and prospect of seed manure fertilizing mechanization in China (国内种肥施肥机械化发展现状及思考). *Journal of Agricultural Mechanization Research*, Vol. 12, pp.1-5, Heilongjiang/China.

[18] Zha, X., Zhang, G., Zhang, S., Hou, Q., Wang, Y., & Zhou, Y. (2020). Design and experiment of centralized pneumatic deep precision fertilization device for rice transplanter. *International Journal of Agricultural and Biological Engineering*, Vol. *13*(6), pp. 109-117. America